



Contents lists available at ScienceDirect

## Journal of Ginseng Research

journal homepage: <http://www.ginsengres.org>

## Research Article

## Ginseng-plus-Bai-Hu-Tang ameliorates diet-induced obesity, hepatic steatosis, and insulin resistance in mice

Hsu-Feng Lu<sup>1,2,☆</sup>, Yu-Heng Lai<sup>3,☆</sup>, Hsiu-Chen Huang<sup>4</sup>, I-Jung Lee<sup>5</sup>, Lie-Chwen Lin<sup>6</sup>, Hui-Kang Liu<sup>6,7</sup>, Hsiao-Hsuan Tien<sup>8</sup>, Cheng Huang<sup>8,9,\*</sup><sup>1</sup> Departments of Clinical Pathology, Cheng Hsin General Hospital, Taipei, Taiwan<sup>2</sup> Department of Restaurant, Hotel and Institutional Management, Fu-Jen Catholic University, New Taipei, Taiwan<sup>3</sup> Department of Chemistry, Chinese Culture University, Taipei, Taiwan<sup>4</sup> Department of Applied Science, National Tsing Hua University South Campus, Hsinchu, Taiwan<sup>5</sup> Department of Kampo Medicine, Yokohama University of Pharmacy, Kanagawa, Japan<sup>6</sup> National Research Institute of Chinese Medicine, Ministry of Health and Welfare, Taipei, Taiwan<sup>7</sup> Ph.D. Program in Clinical Drug Development of Chinese Herbal Medicine, Taipei Medical University, Taipei, Taiwan<sup>8</sup> Department of Biotechnology and Laboratory Science in Medicine, National Yang-Ming University, Taipei, Taiwan<sup>9</sup> Department of Earth and Life Sciences, University of Taipei, Taipei, Taiwan

## ARTICLE INFO

## Article history:

Received 26 April 2018

Received in Revised form

17 August 2018

Accepted 22 October 2018

Available online 27 October 2018

## Keywords:

diet-induced obesity  
ginseng-plus-Bai-Hu-Tang  
hepatic steatosis  
insulin resistance  
*Panax ginseng*

## ABSTRACT

**Background:** Dietary fat has been suggested to be the cause of various health issues. Obesity, hypertension, cardiovascular disease, diabetes, dyslipidemia, and kidney disease are known to be associated with a high-fat diet (HFD). Obesity and associated conditions, such as type 2 diabetes mellitus and nonalcoholic fatty liver disease (NAFLD), are currently a worldwide health problem. Few prospective pharmaceutical therapies that directly target NAFLD are available at present. A Traditional Chinese Medicine, ginseng-plus-Bai-Hu-Tang (GBHT), is widely used by diabetic patients to control glucose level or thirst. However, whether it has therapeutic effects on fat-induced hepatic steatosis and metabolic syndrome remains unclear.

**Methods:** This study was conducted to examine the therapeutic effect of GBHT on fat-induced obesity, hepatic steatosis, and insulin resistance in mice.

**Results:** GBHT protected mice against HFD-induced body weight gain, hyperlipidemia, and hyperglycemia compared with mice that were not treated. GBHT inhibited the expansion of adipose tissue and adipocyte hypertrophy. No ectopic fat deposition was found in the livers of HFD mice treated with GBHT. In addition, glucose intolerance and insulin sensitivity in HFD mice was also improved by GBHT.

**Conclusion:** GBHT prevents changes in lipid and carbohydrate metabolism in a HFD mouse model. Our findings provide evidence for the traditional use of GBHT as therapy for the management of metabolic syndrome.

© 2018 The Korean Society of Ginseng, Published by Elsevier Korea LLC. This is an open access article under the CC BY-NC-ND license (<http://creativecommons.org/licenses/by-nc-nd/4.0/>).

## 1. Introduction

It is well-known that a high-caloric diet, which is rich in carbohydrates and fat, can lead to various health issues, such as obesity, hypertension, cardiovascular disease, diabetes,

dyslipidemia, and kidney disease [1–3]. Dysregulation of insulin action in the liver is strongly associated with these symptoms and is now a worldwide health problem [4]. Nonalcoholic fatty liver disease (NAFLD) is a common metabolic symptom caused by an imbalance of lipid metabolism; patients with long-term NAFLD may

**Abbreviations:** GBHT, Ginseng-plus-Bai-Hu-Tang; NAFLD, Nonalcoholic fatty liver disease; HFD, High-fat diet; NASH, Nonalcoholic steatohepatitis; HDL, High-density lipoprotein; T2DM, Type 2 diabetes mellitus.

\* Corresponding author. Department of Biotechnology and Laboratory Science in Medicine, National Yang-Ming University, No. 155, Sec. 2, Linong St., Beitou District, Taipei 11221, Taiwan.

E-mail address: [chengh@ym.edu.tw](mailto:chengh@ym.edu.tw) (C. Huang).

☆ These authors contributed equally.

<https://doi.org/10.1016/j.jgr.2018.10.005>

p1226-8453 e2093-4947/\$ – see front matter © 2018 The Korean Society of Ginseng, Published by Elsevier Korea LLC. This is an open access article under the CC BY-NC-ND license (<http://creativecommons.org/licenses/by-nc-nd/4.0/>).

progress to an inflammatory subtype, nonalcoholic steatohepatitis (NASH), which has great potential to develop into hepatic fibrosis, leading to cirrhosis and other advanced liver diseases [5]. NAFLD patients are also at high risk of type 2 diabetes mellitus (T2DM), which is associated with the pathological characteristics of excess adiposity and insulin resistance [6–8]. Current therapies for fatty liver disease are aimed at reducing body weight and improving insulin sensitivity to alleviate the associated metabolic syndrome [9,10]. No pharmacotherapy that targets NAFLD has received general approval. Therefore, most NAFLD patients have been directed to treat the individual symptoms of metabolic syndrome, such as obesity, diabetes, hypertension, and dyslipidemia [5].

Bai-Hu-Tang (BHT), composed of *Anemarrhena asphodeloides* Bunge (Zhi-Mu), Gypsum fibrosum (Shi-Gao; inorganic CaSO<sub>4</sub>), root of *Glycyrrhiza uralensis* Fisch. (Gan-Cao), as seed of *Oryza sativa* L. (Jing-Mi), is a Traditional Chinese Medicine described in the Chinese medicine book “Discussion of Cold Damage” (“Shang-Han-Lun” in Chinese), which has been used in China for over 1800 years. BHT potentiates insulin-stimulated glucose uptake *in vitro* [11]. The formula used in this study was ginseng-plus-Bai-Hu-Tang (GBHT), which is an enhanced formula of BHT prepared by addition of *Panax ginseng* Meyer. GBHT is the most common herbal formula prescribed by Traditional Chinese Medicine doctors for the treatment of T2DM [12]. Previously, GBHT has been reported to have significant antihyperglycemic activity [13]. In addition, we reported the treatment of diabetic dyslipidemia with GBHT [14]. However, whether it has a therapeutic effect on fat-induced hepatic steatosis and metabolic syndrome remains unclear.

In this study, we used the high-fat diet (HFD) C57BL/6J mouse model to investigate the clinical effects of GBHT on fat-induced hepatic steatosis and insulin resistance. We found that the mice displayed clear symptoms of dyslipidemia and abnormality of glucose metabolism and expressed markers of hepatic steatosis under a HFD. This suggests that the model may be valuable for studying the effect of GBHT on diet-induced obesity, dyslipidemia, and liver-related metabolic syndrome.

## 2. Materials and methods

### 2.1. GBHT formula and preparation

GBHT is composed of five crude ingredients with root of *P. ginseng* (Ren Shen), rhizome of *A. asphodeloides* Bunge (Zhi-Mu), Gypsum fibrosum (Shi-Gao; inorganic CaSO<sub>4</sub>), root of *G. uralensis* Fisch. (Gan-Cao), and seed of *O. sativa* L. (Jing-Mi). To confirm the identity of the five ingredients of GBHT, all the specimens were sliced manually by hand, fixed in a solution of 50% glycerin in water, and observed under a microscope (Carl Zeiss Inc., Germany). The GBHT powder was prepared as described previously [14]. In brief, GBHT was prepared in a classical dosage ratio used in the traditional Chinese era (3 parts *P. ginseng*, 6 parts by weight of *A. asphodeloides* Bunge, 16 parts Gypsum fibrosum, 2 parts *G. uralensis* Fisch., and 8 parts *O. sativa* L.). To prepare the water extracts, 35 g of the mixture or the corresponding weight of each single ingredient (e.g. 3 g of *P. ginseng*) was added to 400 ml of water and refluxed at 100°C for 1 h, then the supernatant was collected, clarified by centrifugation at 1000 g for 10 min at 4°C, and either used directly or lyophilized and dissolved in ddH<sub>2</sub>O in animal experiments.

### 2.2. High performance liquid chromatography sample preparation

The dried GBHT powder (0.5 g) was dissolved in 5 mL of 70% MeOH, then filtered through a 0.45 μm syringe filter, and a volume of 20 μL of filtrate was used for analysis. Stock solutions of

ginsenoside Rg1, ginsenoside Rg3, mangiferin (M), glycyrrhizic acid (GA), liquiritin apioside (LA), and liquiritin (L) in MeOH (2 mg/mL) were prepared. A mixed standard solution containing the six compounds was prepared by diluting them with 70% MeOH to obtain a concentration of 200 μg/mL of each component. Working standard solutions were prepared by diluting the mixed standard solution with 70% MeOH to give the concentrations 100, 60, 50, 20, and 10 μg/mL of each component; these were used for the validation and to produce the calibration curves.

### 2.3. High performance liquid chromatography analysis

High performance liquid chromatography (HPLC) analyses were performed on a Shimadzu-HPLC system comprising a chromatographic pump (LC-20AT), an autosampler (SIL-20A) equipped with a 100 μL sample loop, and a photodiode array detector (SPD-M20A) controlled by LabSolution software. A Purospher® STAR RP-18e column (4.6 × 250 mm, 5 μm, Merck, Darmstadt, Germany) was used to analyze the samples. The mobile phase consisted of A solvent: water (with 0.001% H<sub>3</sub>PO<sub>4</sub>) and B solvent: acetonitrile (with 0.001% H<sub>3</sub>PO<sub>4</sub>). An eluting program was set, from 10% B to 55% B over 0 min to 35 min, maintaining 55% B to 40 min, increasing to 90% B from 40 min to 41 min, and then maintaining 90% B to 50 min, all at a flow rate of 1.0 μL/min. The injection volume was 20 μL. DAD detection was performed in the 200–600 nm range, and the recorder wavelengths were set at 203 nm (for ginsenoside Rg1 and ginsenoside Rg3), 254 nm (for M and GA), and 276 nm (for LA and L).

### 2.4. Calibration curves

Five concentrations (10, 20, 50, 60, and 200 mg/mL) of the mixed standard solution were injected in triplicate (Table 1), and their regression equations were calculated in the form of  $y = Ax + B$ . The following are the results: ginsenoside Rg1,  $y = 5857.3x - 15769$ ,  $r^2 = 0.9997$ ; ginsenoside Rg3,  $y = 7975.2x - 23491$ ,  $r^2 = 0.9998$ ; M,  $y = 78287x - 211564$ ,  $r^2 = 0.9997$ ; GA,  $y = 10746x - 22914$ ,  $r^2 = 0.9998$ ; LA,  $y = 19231x - 57237$ ,  $r^2 = 0.9998$ ; and L,  $y = 39549x - 79948$ ,  $r^2 = 0.9999$ . Data are expressed as the mean ± standard deviation from three independent experiments.

### 2.5. Animals

Thirty 4-week-old male C57BL/6J mice were purchased from The National Laboratory Animal Center, Taipei, Taiwan. All mice were housed individually under a constant temperature (24°C) and 12 h light/dark cycle at the Animal Center of the National Research Institute of Chinese Medicine, Taipei, Taiwan. The use of animals for this research was approved by the Animal Research Committee of the National Research Institute of Chinese Medicine (IACUC no. 105-520-1), and all procedures followed The Guide for the Care and Use of Laboratory Animals (NIH publication, 85-23, revised 1996) and the guidelines of the Animal Welfare Act, Taiwan. Mice fed with a standard diet and adapted to the environment for 1 week were subsequently divided randomly into three groups and fed a normal diet (ND, n = 10), HFD (n = 10, 30% fat and 1% cholesterol), or HFD with 0.5% (w/w) GBHT (n = 10) for 12 weeks. All experimental diets were prepared weekly and stored at –20°C. At the end of the experimental period, serum samples were collected before sacrifice. The liver tissue and epididymis adipose tissue (EAT) were harvested for further analysis.

### 2.6. Histological analyses of the liver and fat tissues

The liver and EAT were removed from each mouse. Samples were subsequently fixed in 10% paraformaldehyde/PBS and

**Table 1**  
Precision and accuracy of the HPLC-UV method for the determination of standards ginsenoside Rg1, ginsenoside Rg3, mangiferin, glycyrrhizic acid, liquiritin apioside, and liquiritin

Ginsenoside Rg1		Ginsenoside Rg3			Mangiferin				
Nominal conc. (µg/mL)	Observed conc. (µg/mL)	Precision (RSD, %)	Accuracy (Bias, %)	Observed conc. (µg/mL)	Precision (RSD, %)	Accuracy (Bias, %)	Observed conc. (µg/mL)	Precision (RSD, %)	Accuracy (Bias, %)
10	11.32 ± 0.04	0.37	-11.69	11.64 ± 0.04	0.38	-14.12	11.73 ± 0.25	2.14	-14.78
20	19.89 ± 0.04	0.18	0.57	19.64 ± 0.11	0.55	1.82	19.57 ± 0.02	0.10	2.21
50	50.41 ± 0.35	0.69	-0.81	48.98 ± 0.11	0.22	2.08	50.32 ± 0.13	0.25	-0.64
60	57.91 ± 2.61	4.51	3.61	59.32 ± 1.04	1.75	1.15	57.86 ± 2.25	3.88	3.71
200	200.47 ± 0.62	0.31	-0.23	200.41 ± 1.43	0.71	-0.21	200.52 ± 0.02	0.01	-0.26

Glycyrrhizic acid		Liquiritin apioside			Liquiritin				
Nominal conc. (µg/mL)	Observed conc. (µg/mL)	Precision (RSD, %)	Accuracy (Bias, %)	Observed conc. (µg/mL)	Precision (RSD, %)	Accuracy (Bias, %)	Observed conc. (µg/mL)	Precision (RSD, %)	Accuracy (Bias, %)
10	11.06 ± 0.08	1.95	-10.88	11.06 ± 0.08	0.71	-9.55	11.44 ± 0.41	3.61	-12.58
20	19.95 ± 0.29	0.22	2.77	19.95 ± 0.29	1.47	0.26	19.93 ± 0.35	1.75	0.35
50	51.17 ± 0.12	0.26	-1.50	51.17 ± 0.12	0.24	-2.28	50.90 ± 0.11	0.21	-1.78
60	57.38 ± 0.66	4.17	3.06	57.38 ± 0.66	1.15	4.56	57.17 ± 1.49	2.60	4.96
200	200.45 ± 2.71	0.20	-0.17	200.45 ± 2.71	1.35	-0.22	200.56 ± 0.57	0.28	-0.28

embedded in paraffin or frozen for staining with hematoxylin and eosin or with Oil red O (ORO). All specimens were observed microscopically (Carl Zeiss Inc., Germany) at 200 × magnification.

### 2.7. Biochemical analysis of plasma

The plasma triglyceride (TG), total cholesterol (TC), high-density lipoprotein-cholesterol (HDL-C), glutamic oxaloacetic transaminase (GOT), glutamic pyruvic transaminase (GPT), lactic dehydrogenase, total bilirubin, uric acid, and lipase levels were measured using enzymatic assay kits with a FUJI DRI-CHEM analyzer (Fujifilm, Tokyo, Japan). The non-HDL-C level was calculated as [(TC) - (HDL-C) - (TG/5)].

### 2.8. Blood glucose, plasma insulin, the homeostasis model assessment of insulin resistance index, and intraperitoneal glucose tolerance test

Every 2 weeks, the 12 h fasting blood glucose was measured in tail vein blood with a glucose analyzer (EASYS TOUCH, Miaoli County, Taiwan). An enzymatic assay was used to measure the plasma insulin concentration (Cisbio, MA, USA). The homeostasis model assessment of insulin resistance (HOMA-IR) was calculated as [fasting insulin concentration (mU/L) × fasting glucose concentration (mg/dL) × 0.05551]/22.5. For the intraperitoneal glucose tolerance test, the analysis was performed during the 12th week after the start of the diet experiments, mice fasted for 12 h were

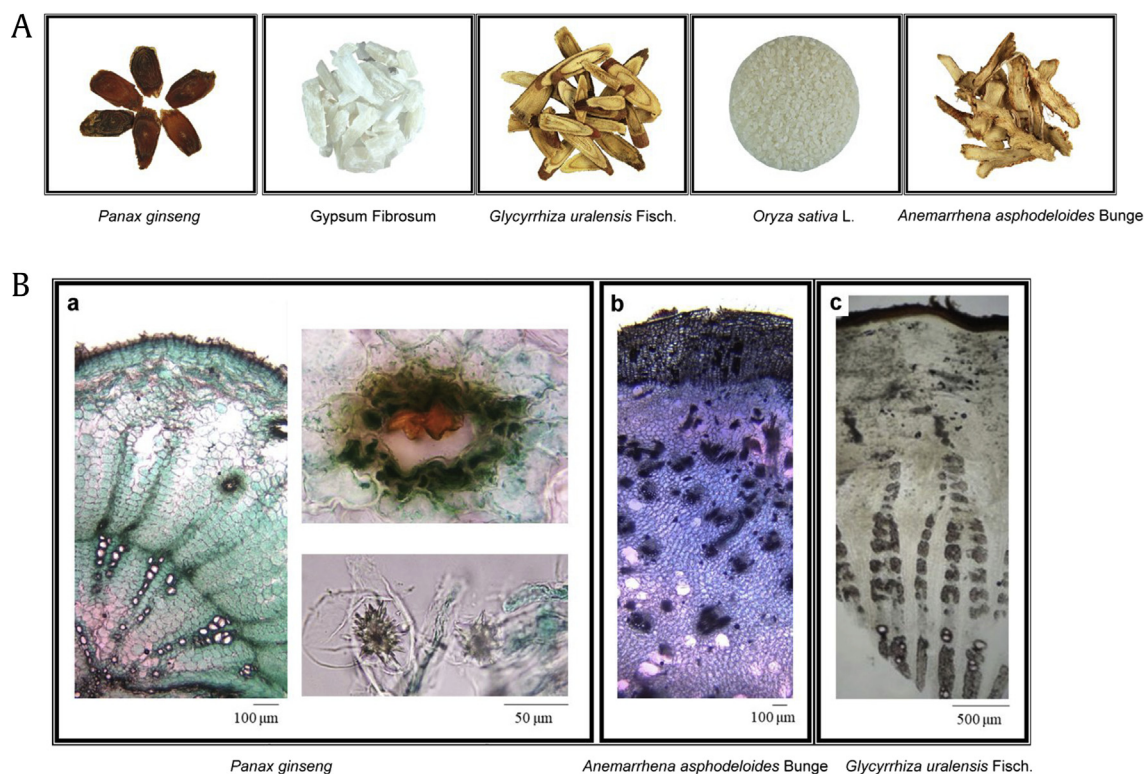


**Fig. 1.** The macroscopic appearance of the five herbs used to prepare GBHT was examined. (A) Specimens of the five herbs are shown. (B) The microscopic appearance of the *P. ginseng* (a), *Anemarrhena asphodeloides* Bunge (b), and *Glycyrrhiza uralensis* Fisch. (c). GBHT, ginseng-plus-Bai-Hu-Tang.

injected intraperitoneally with glucose (1 g/kg body weight), and the blood glucose level was determined in tail vein blood at 0, 30, 60, 90, and 120 min after glucose injection.

### 2.9. Statistical analysis

All values are expressed as the mean  $\pm$  standard deviation from at least three separate experiments. Area under the curve analysis was performed using the trapezoidal method. One-way analysis of variance followed by Dunnett's multiple comparison test was used to compare differences among groups of samples. Asterisks indicated that the values were significantly different from the control ( $*p < 0.05$ ;  $**p < 0.01$ ).

## 3. Results

### 3.1. Characterization of the five ingredients of GBHT

GBHT is composed of five crude ingredients: root of *P. ginseng* (Ren Shen), rhizome of *A. asphodeloides* Bunge (Zhi-Mu), Gypsum fibrosum (Shi-Gao, inorganic  $\text{CaSO}_4$ ), root of *G. uralensis* Fisch. (Gan-Cao), and seed of *O. sativa* L. (Jing-Mi). The appearance and microscopic features of each ingredient were confirmed (Fig. 1A and B). In microscopic identification, the transverse section of the *P. ginseng* was cork consisting of several rows of cells and phloem, showing clefts outside (Fig. 1B, panel a). The transverse section of the dried *A. asphodeloides* Bunge showed cork consisting of several

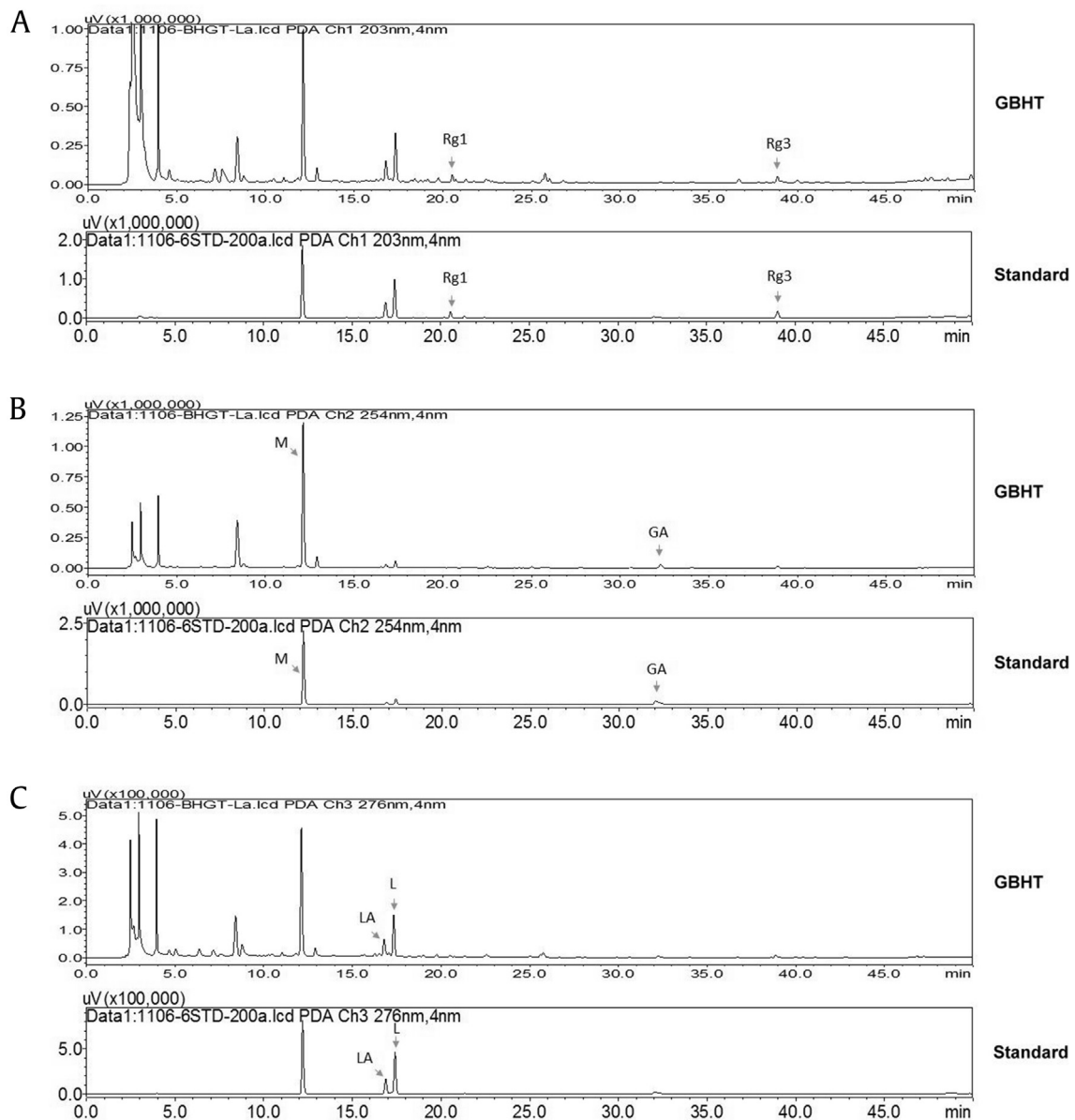


**Fig. 2.** HPLC analysis and LC-UV chromatogram of GBHT. The HPLC analysis was performed in a reverse-phase column C18, gradient mobile system of acetonitrile in 0.001% phosphoric acid, flow rate set at 1.0 mL/min, and an LC-UV chromatogram of GBHT was recorded at UV 203 nm (A, upper panel), UV 254 nm (B, upper panel), and UV 276 nm (C, upper panel). Representative LC-UV chromatograms of standards of mangiferin, ginsenoside Rg1, ginsenoside Rg3, glycyrrhizic acid, liquiritin apioside, and liquiritin that were recorded at UV 203 nm (A, lower panel), UV 254 nm (B, lower panel), and UV 276 nm (C, lower panel). GBHT, ginseng-plus-Bai-Hu-Tang; GA, glycyrrhizic acid; HPLC, high performance liquid chromatography; LA, liquiritin apioside; L, liquiritin; M, mangiferin; Rg1, ginsenoside Rg1; Rg3, ginsenoside Rg3.

to over 30 rows of cells and spiral or vessels about 10~50  $\mu\text{m}$  (Fig. 1B, panel b). The transverse section of *G. uralensis* Fisch. was cork consisting of several layers of brown cells, and the cortex was relatively narrow (Fig. 1B, panel c).

### 3.2. Development of an HPLC-UV analytical method to determine the identity and consistency of GBHT

An HPLC-UV analytical method was developed to determine the identity and consistency of GBHT. As shown in Fig. 2, a high-resolution chemical fingerprint of GBHT was obtained. Quantitative analyses of the marker compounds ginsenoside Rg1 and ginsenoside Rg3 (key principles of *P. ginseng*); M (key principle of *A. asphodeloides* Bunge); and L, LA, and GA (key principles of *G. uralensis* Fisch.) were performed, and representative HPLC chromatograms are shown. Calibration curves were established at concentrations of 10, 20, 50, 60, and 200  $\mu\text{g}/\text{mL}$ . Correlated linear relationships were obtained for all standards, with a coefficient of estimation  $r^2 > 0.9995$ . The accuracy (% bias) and precision (% RSD) values of the six standards are presented in Table 1, and all percentages for the bias and RSD values are within 15% and acceptable for this quantification method. This validated method was used to analyze the GBHT sample. The contents of the GBHT sample were  $1.05 \pm 0.01$  mg/g (M),  $0.67 \pm 0.02$  mg/g (L),  $0.84 \pm 0.00$  mg/g (LA),  $0.37 \pm 0.01$  mg/g (GA),  $0.75 \pm 0.01$  mg/g (ginsenoside Rg1), and  $0.51 \pm 0.00$  mg/g (ginsenoside Rg3).

### 3.3. GBHT lowered weight of body and food efficiency ratio in HFD mice

Our previous study confirmed the inhibitory effect of GBHT on the accumulation of palmitate-induced cellular lipid through the AMP-activated protein kinase (AMPK) pathway [14]. Therefore, we examined the effect of GBHT on fatty liver and lipemia syndrome in our HFD mouse model. Five-week-old male C57BL/6J mice were fed a HFD along with or without 0.5% GBHT for 12 weeks. The HFD mice were significantly heavier than the ND and HFD-GBHT mice after 12 weeks of diet (Fig. 3A). Also, we observed that GBHT lowered the food efficiency (Fig. 3B). This inferred that the HFD mice have a sign of metabolic syndrome, with the main characteristics of central obesity with fat accumulation around the waist, and the GBHT treatment significantly inhibited an increase in body weight and food efficiency ratio compared with the HFD group.

### 3.4. GBHT inhibits fat deposition in adipocytes in HFD mice

A feature of metabolic syndrome is increasing fat within the trunk region, caused by excessive visceral fat deposits. Next, we dissected and measured the size of the EAT as a criterion. The mass of EAT in the HFD group was significantly greater than the ND group (Fig. 4A). In contrast, the HFD-GBHT mice had a smaller EAT mass. The size of the adipocytes was measured in each group (Fig. 4B and C). ORO staining was used to identify the neutral lipid and fatty acid contents, a red color indicating intracellular triglycerides. A substantial amount of intracellular lipid was stained by ORO in the EAT section in the HFD group. GBHT administration significantly reduced such intracellular lipid accumulation. Compared with adipocytes from the HFD group, the GBHT-fed group showed a lower EAT adipocyte diameter, size, and lipid content, which suggested that GBHT may inhibit fat deposition in HFD mice.

### 3.5. Hyperlipemia was prevented by GBHT treatment in HFD mice

Because it is well known that alteration of the lipid composition in serum is a sign of metabolic deficiency [15,16], we profiled the

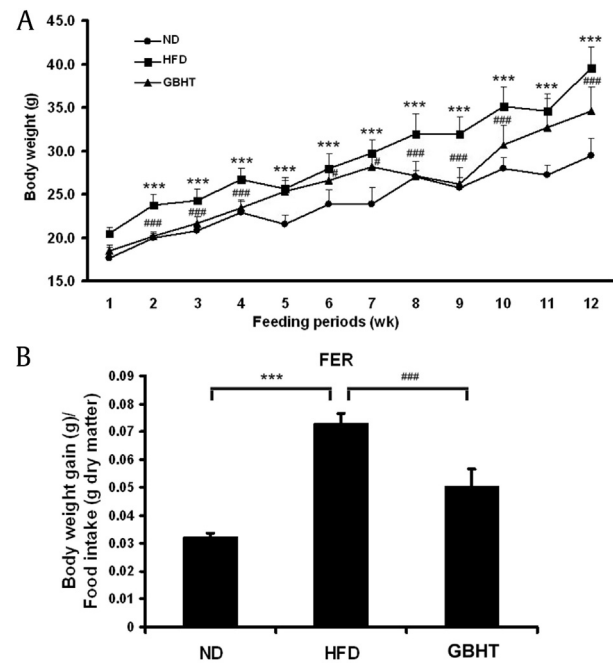


**Fig. 3.** The effect of GBHT on body weights and food efficiency ratio in C57BL/6J mice fed an HFD. (A) Changes in body weight. (B) Food efficiency ratio (FER). Data are shown as means  $\pm$  SEM. ND vs. HFD: \* $p < 0.05$ ; \*\* $p < 0.01$ ; \*\*\* $p < 0.001$ . HFD vs. GBHT: # $p < 0.05$ ; ## $p < 0.01$ ; ### $p < 0.001$ .

GBHT, ginseng-plus-Bai-Hu-Tang; HFD, high-fat diet; ND, normal diet; SEM, standard error of mean.

plasma lipid levels in our mouse model. Plasma TG, TC, HDL-C, and non-HDL-C were measured, revealing significantly high TG, TC, and non-HDL-C in the HFD group (Fig. 5A, B, and D). The TG, TC, and non-HDL-C were significantly lower in the HFD-GBHT group than the HFD group, except for HDL-C (Fig. 5C). The results indicate that GBHT prevented an increase of plasma lipid levels in HFD mice.

### 3.6. GBHT inhibited HFD-induced intracellular lipid accumulation in the liver

Fatty liver disease is mainly attributable to triglyceride accumulation in hepatocytes [17]. To determine whether lipid accumulation in hepatocytes is inhibited by GBHT, using the HFD mouse model, we examined the liver weight and morphology to observe lipid deposition and accumulation with hematoxylin and eosin staining. We first weighed the livers and found those of the HFD group were heavier than the ND group (Fig. 6A). The liver weight was significantly lower in the HFD-GBHT mice than the HFD group. In addition, the hepatocytes of the HFD mice were swollen and larger in size, with a foaming morphology and lack of staining, suggesting more lipid deposition (Fig. 6B). The increased size of the hepatocytes reduced the diameter of the central vein and diminished the sinusoids. Interestingly, tissue morphology revealed that intracellular lipid accumulation was lower in the GBHT group than the HFD group.

### 3.7. GBHT inhibited increase in the levels of hepatic steatosis-related markers under high fat conditions

Generally, hepatic steatosis was considered to be a common feature of nonalcoholic fatty liver patients [18]. Several hepatic-steatosis markers were examined to determine the effect of GBHT on HFD-induced steatohepatitis. The levels of aspartate

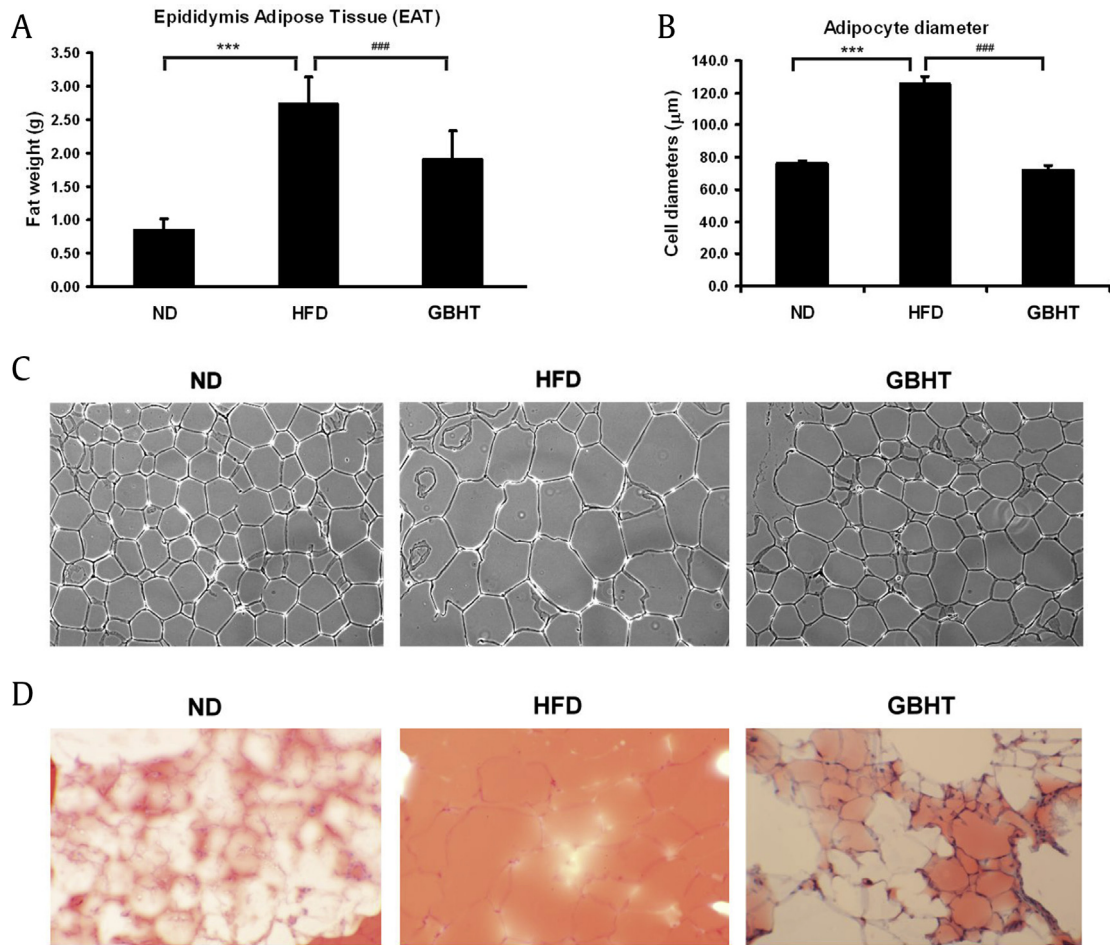


**Fig. 4.** The effect of GBHT on fat deposition in C57BL/6j mice fed an HFD. (A) The weight of epididymis adipose tissue (EAT). (B) The adipocytes diameters were measured. (C) Hematoxylin-eosin staining showed adipocytes in the EAT of the mice. (D) Oil-red O staining showed lipid contents in the EAT of the mice. Data are shown as means  $\pm$  SEM. ND vs. HFD:  $***p < 0.001$ . HFD vs. GBHT:  $###p < 0.001$ . GBHT, ginseng-plus-Bai-Hu-Tang; HFD, high-fat diet; ND, normal diet; SEM, standard error of mean.

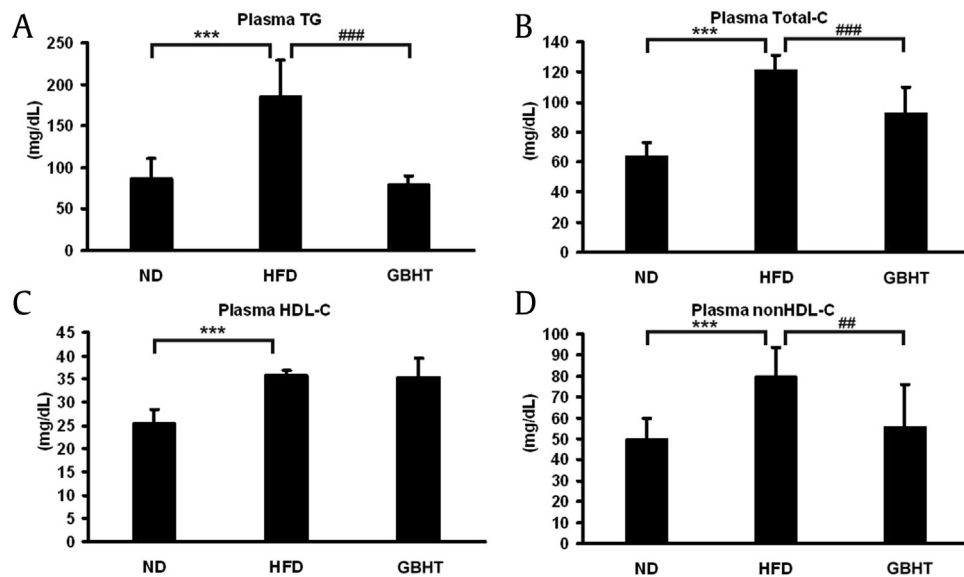


**Fig. 5.** The effect of GBHT on plasma lipid levels in C57BL/6j mice fed an HFD. (A) The levels of plasma TG. (B) The levels of total-C. (C) The levels of HDL-C. (D) The levels of non-HDL-C. Data are shown as means  $\pm$  SEM. ND vs. HFD:  $***p < 0.001$ . HFD vs. GBHT:  $##p < 0.01$ ;  $###p < 0.001$ . GBHT, ginseng-plus-Bai-Hu-Tang; HFD, high-fat diet; ND, normal diet; SEM, standard error of mean; TG, triglyceride; HDL-C, high-density lipoprotein-cholesterol.

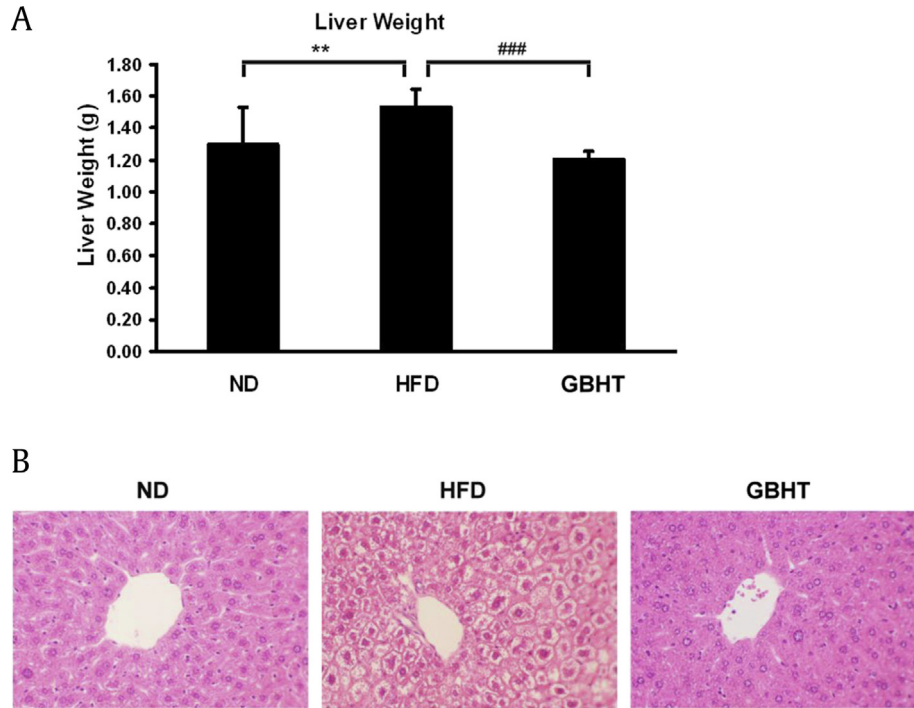


**Fig. 6.** The effect of GBHT on lipid accumulation in the livers of C57BL/6 mice fed an HFD. (A) Changes in liver weight. Data are shown as means  $\pm$  SEM. ND vs. HFD: \*\* $p < 0.01$ . HFD vs. GBHT: ### $p < 0.001$ . (B) Hematoxylin and eosin staining of transverse liver sections (original magnification  $\times 200$ ). GBHT, ginseng-plus-Bai-Hu-Tang; HFD, high-fat diet; ND, normal diet; SEM, standard error of mean.

aminotransferase (AST/GOT) and alanine aminotransferase (ALT/GPT), as well as lactate dehydrogenase and total bilirubin, in serum can help diagnose injury to hepatic tissue [19,20]. These markers of hepatic lipotoxicity were upregulated in HFD mice but were significantly lower in the GBHT-treated HFD mice (Fig. 7A–D). Also, GBHT significantly inhibited increases in the marker for renal disease, uric acid [21], which was much higher in the HFD group (Fig. 7E). Finally, we examined the marker of acute pancreatitis, lipase, and found no differences among the three groups (Fig. 7F). This suggests that HFD and GBHT uptake may not cause serious

injury to the pancreas. To sum up, a HFD-induced steatohepatitis and kidney damage and GBHT showed a significant effect in preventing the syndrome.

### 3.8. GBHT prevented HFD-induced insulin resistance and glucose tolerance

It has been reported that hyperglycemia tends to develop in mice within 4 weeks of a HFD [22]. Moreover, the high-fasting insulin level is considered to be the earliest clinical reaction during

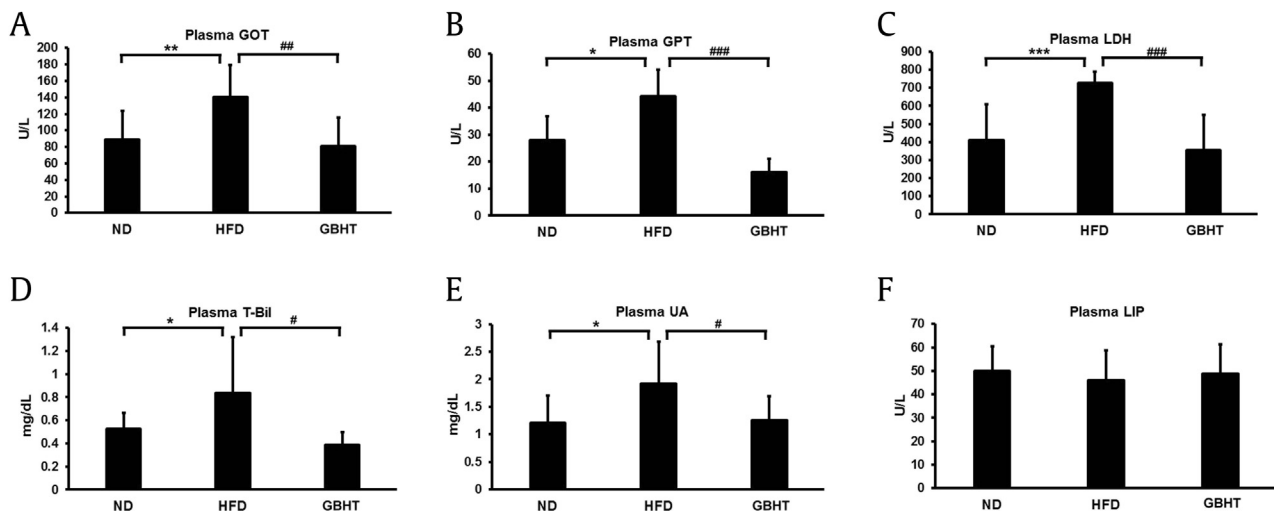


**Figure 7**

**Fig. 7.** The effect of GBHT extract treatment on the levels of hepatic steatosis-related markers in C57BL/6 mice fed an HFD. (A–D) The plasma levels of the hepatic lipotoxicity markers GOT, GPT, LDH, and total bilirubin. (E) The plasma levels of the kidney lipotoxicity markers UA. (F) The plasma levels of the pancreas lipotoxicity marker lipase (LIP). Data are shown as means  $\pm$  SEM. ND vs. HFD: \* $p < 0.05$ ; \*\* $p < 0.01$ ; \*\*\* $p < 0.001$ . HFD vs. GBHT: # $p < 0.05$ ; ## $p < 0.01$ ; ### $p < 0.001$ . GBHT, ginseng-plus-Bai-Hu-Tang; GOT, glutamic pyruvic transaminase; GPT, glutamic pyruvic transaminase; HFD, high-fat diet; LDH, lactic dehydrogenase; ND, normal diet; SEM, standard error of mean; UA, uric acid.

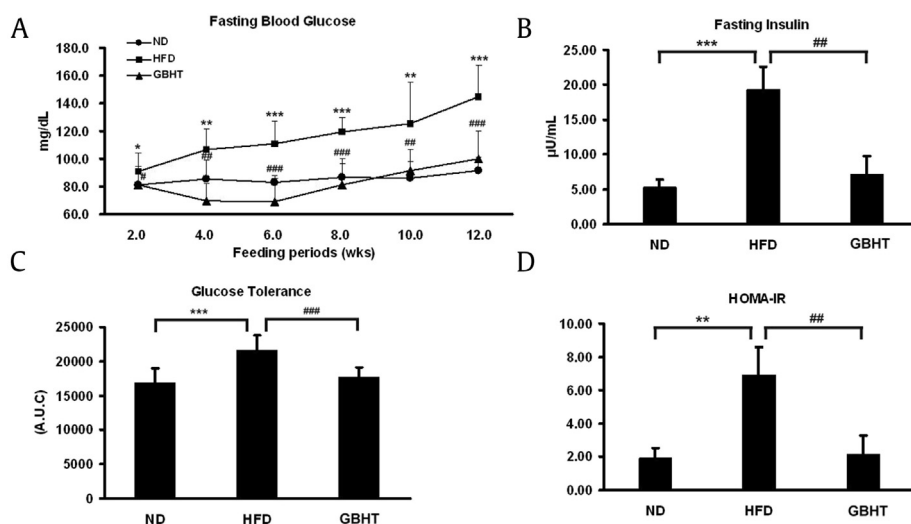


**Fig. 8.** The effect of GBHT on glucose metabolism and insulin resistance in C57BL/6J mice fed an HFD. (A) Blood glucose levels after 12 h of fasting. (B) Plasma insulin levels after 12 h of fasting. (C) Area under the curve (AUC) of blood glucose and insulin levels. (D) The HOMA-IR index calculated using fasting blood glucose and insulin levels. Data are shown as means  $\pm$  SEM. ND vs. HFD: \* $p < 0.05$ ; \*\* $p < 0.01$ ; \*\*\* $p < 0.001$ . HFD vs. GBHT: # $p < 0.05$ ; ## $p < 0.01$ ; ### $p < 0.001$ . GBHT, ginseng-plus-Bai-Hu-Tang; HFD, high-fat diet; HOMA-IR, homeostasis model assessment of insulin resistance; ND, normal diet; SEM, standard error of mean.

metabolic syndrome [23]. We measured the fasting blood glucose and insulin levels in HFD-C57BL/6J mice with or without GBHT. The high fasting blood glucose level in the GBHT group was significantly lower than the HFD group (Fig. 8A). The plasma insulin level was 4-fold higher in the HFD mice but inhibited by GBHT (Fig. 8B). The IPGTT revealed that GBHT significantly improved glucose tolerance (Fig. 8C). The HOMA-IR index was calculated and found to be at the control level with GBHT treatment (Fig. 8D), indicating inhibition of insulin resistance.

#### 4. Discussion

Phytomedicine, with antiobesity, hypolipidemic, and antidiabetic effects, has been widely used throughout history. One common herbal treatment, GBHT, which is an enhanced formula of BHT prepared by addition of *P. ginseng* (Ren Shen), has been used to reduce the symptoms of thirst in T2DM patients [12]. Ginsenoside Rb1 (Rb1), a compound extracted from ginseng root, significantly reduces body weight, improves glucose tolerance, and enhances insulin action in HFD-induced obese rats [24] and has a glucose-lowering action in vitro [25]. A water extract of ginseng root was found to have a fat-lowering action *in vivo* [26]. Using the model we reported previously, we showed that GBHT reduced total lipid and triglyceride accumulation in hepatocytes by upregulating AMPK and downregulating acetyl-CoA carboxylase signaling [14]. Therefore, in this study, we sought to determine whether GBHT could prevent hepatic fat accumulation associated with obesity and to evaluate the therapeutic effects of GBHT in metabolic syndrome.

Using our model, we found that mice with a HFD experienced significant weight increase, lipid accumulation within liver, dyslipidemia, steatohepatitis, and insulin resistance. These symptoms are consistent with a previous study that identified metabolic syndrome [27]. The presence of hypertriglyceridemia and high cholesterol is consistent with the symptoms of obesity and diabetes in humans [28,29], suggesting that the HFD mouse model is suitable as an animal model of metabolic syndrome and for investigation of the bioactivity of GBHT. Interestingly, when GBHT was administered to mice under a HFD, metabolic abnormalities were significantly prevented. GBHT blocked the storage of total fat in EAT and liver and prevented increases in triglycerides and cholesterol in

the plasma, which consequently diminished the organ weight. This suggests that the inhibitory effect of GBHT on lipid metabolism is applicable to HFD-induced metabolic syndrome.

GBHT is the most common herbal formula prescribed by Traditional Chinese Medicine doctors for the treatment of T2DM [12] and has been reported to have antihyperglycemic activity [13]. In fact, impaired glucose tolerance has a great probability of developing into T2DM [30] in obese patients. Generally, insulin resistance is calculated using HOMA-IR [23], and increased HOMA-IR values have a great impact on T2DM incidence in the human population [31]. While a HFD increased the symptoms of diabetes, such as high fasting blood glucose, insulin level, glucose tolerance, and HOMA-IR value, in HFD mice, when the mice were treated with GBHT, along with the HFD, the high blood glucose and insulin resistance were ameliorated.

On the other hand, a high HDL-C level was detected in both the HFD and HFD-GBHT groups and may be attributable to the high cholesterol diet. However, the high level of non-HDL-C, usually referred to as a "bad" cholesterol transportation carrier, was considered as a harmful sign in the HFD group, and GBHT efficiently prevented an increase of non-HDL-C in our mouse model. In addition, insulin resistance has been associated with a HFD and is accompanied by obesity in rodent models [32,33]. Moreover, a HFD has been suggested to be a potential positive regulator of DNA methylation in genes that are associated with energy homeostasis in adipocytes [34]. Therefore, we suggest that GBHT may modulate lipid and carbohydrate metabolism and be able to restore homeostasis. Although we have proved that GBHT reduced fatty liver through an AMPK-activating mechanism in a mouse model of insulin resistance, the biological mechanism of GBHT in inhibition of HFD-induced metabolic syndrome remains uncertain and should be clarified in the future.

NASH is considered to be a health-threatening, chronic liver disease that can progress to cirrhosis [35]. Histologically, NASH can be diagnosed only by liver biopsy [36]; however, this invasive procedure may not be cost effective and has inherent risks [37]. It has been reported that GOT (AST) and GPT (ALT) are crucial parameters when we consider the incidence of NASH, on the basis of noninvasive serum assays [38]. By measuring markers of steatohepatitis in plasma, we confirmed that the HFD caused severe

NASH-like symptoms. Surprisingly, when GBHT was combined with the HFD, there was less secretion of markers of steatohepatitis, which indicates that the mice were less likely to develop NASH. This not only implies the clinical therapeutic effect of GBHT but also suggests this rodent model may be valuable for screening potential serological markers of NASH. Using such a model for screening may facilitate the diagnostic analysis of life-threatening NASH in the future.

## 5. Conclusion

In summary, we have demonstrated that GBHT prevented changes in lipid and carbohydrate metabolism in a HFD mouse model. Our findings provide evidence for the traditional use of GBHT as therapy for the management of metabolic syndrome.

## Conflicts of interest

The authors have declared no conflict of interest.

## Acknowledgments

This work was supported by research grants MOST104-2320-B-077-003 - and MOST 106-2320-B-077-006 - from the Ministry of Science and Technology, Taiwan.

## Appendix A. Supplementary data

Supplementary data to this article can be found online at <https://doi.org/10.1016/j.jgr.2018.10.005>.

## References

- [1] Johnson RJ, et al. Potential role of sugar (fructose) in the epidemic of hypertension, obesity and the metabolic syndrome, diabetes, kidney disease, and cardiovascular disease. *Am J Clin Nutr* 2007;86(4):899–906.
- [2] Fraulob JC, et al. A mouse model of metabolic syndrome: insulin resistance, fatty liver and non-alcoholic fatty pancreas disease (NAFPD) in C57BL/6 mice fed a high fat diet. *J Clin Biochem Nutr* 2010;46(3):212–23.
- [3] Podrini C, et al. High-fat feeding rapidly induces obesity and lipid derangements in C57BL/6N mice. *Mamm Genome* 2013;24(5–6):240–51.
- [4] Dunn W, et al. Suspected nonalcoholic fatty liver disease and mortality risk in a population-based cohort study. *Am J Gastroenterol* 2008;103(9):2263–71.
- [5] Lam B, Younossi ZM. Treatment options for nonalcoholic fatty liver disease. *Therap Adv Gastroenterol* 2010;3(2):121–37.
- [6] Postic C, Girard J. Contribution of de novo fatty acid synthesis to hepatic steatosis and insulin resistance: lessons from genetically engineered mice. *J Clin Invest* 2008;118(3):829–38.
- [7] Masuoka, H.C. and N. Chalasani, Nonalcoholic fatty liver disease: an emerging threat to obese and diabetic individuals. *Ann N Y Acad Sci*. 1281: p. 106–122.
- [8] Smith, B.W. and L.A. Adams, Nonalcoholic fatty liver disease and diabetes mellitus: pathogenesis and treatment. *Nat Rev Endocrinol*. 7(8): p. 456–465.
- [9] Adams LA, Angulo P. Treatment of non-alcoholic fatty liver disease. *Postgrad Med J* 2006;82(967):315–22.
- [10] Nobili V, et al. Lifestyle intervention and antioxidant therapy in children with nonalcoholic fatty liver disease: a randomized, controlled trial. *Hepatology* 2008;48(1):119–28.
- [11] Chen CC, et al. Peroxisome proliferator-activated receptor gamma transactivation-mediated potentiation of glucose uptake by Bai-Hu-Tang. *J Ethnopharmacol* 2008;118(1):46–50.
- [12] Huang CY, et al. Prescription pattern of Chinese herbal products for diabetes mellitus in taiwan: a population-based study. *Evid Based Complement Alternat Med* 2013;2013:201329.
- [13] Kimura I, et al. The antihyperglycaemic blend effect of traditional Chinese medicine byakko-ka-ninjin-to on alloxan and diabetic KK-Ca(y) mice. *Phytother Res* 1999;13(6):484–8.
- [14] Liu HK, et al. Ginseng-plus-Bai-Hu-Tang decoction reduces fatty liver by activating AMP-activated protein kinase in vitro and in vivo. *Evid Base Compl Alternat Med* 2015;2015:651734.
- [15] Kawamoto TH, et al. Resting metabolic rates of two orbweb spiders: a first approach to evolutionary success of cribellate spiders. *J Insect Physiol* 2011;57(3):427–32.
- [16] Suliga E, et al. Factors associated with adiposity, lipid profile disorders and the metabolic syndrome occurrence in premenopausal and postmenopausal women. *PLoS One* 2016;11(4):e0154511.
- [17] Zambo, V., et al., Lipotoxicity in the liver. *World J Hepatol*. 5(10): p. 550–557.
- [18] Fabbri E, Magkos F. Hepatic steatosis as a marker of metabolic dysfunction. *Nutrients* 2015;7(6):4995–5019.
- [19] Cassidy WM, Reynolds TB. Serum lactic dehydrogenase in the differential diagnosis of acute hepatocellular injury. *J Clin Gastroenterol* 1994;19(2):118–21.
- [20] Dufour DR, et al. Diagnosis and monitoring of hepatic injury. II. Recommendations for use of laboratory tests in screening, diagnosis, and monitoring. *Clin Chem* 2000;46(12):2050–68.
- [21] Giordano C, et al. Uric acid as a marker of kidney disease: review of the current literature. *Dis Markers* 2015;2015:382918.
- [22] Sato A, et al. Antiobesity effect of eicosapentaenoic acid in high-fat/high-sucrose diet-induced obesity: importance of hepatic lipogenesis. *Diabetes* 2010;59(10):2495–504.
- [23] Ling JC, et al. Determinants of high fasting insulin and insulin resistance among overweight/obese adolescents. *Sci Rep* 2016;6:36270.
- [24] Xiong, Y., et al., Antiobesity and antihyperglycemic effects of ginsenoside Rb1 in rats. *Diabetes*. 59(10): p. 2505–2512.
- [25] Park S, et al. Ginsenosides Rb1 and Rg1 suppress triglyceride accumulation in 3T3-L1 adipocytes and enhance beta-cell insulin secretion and viability in Min6 cells via PKA-dependent pathways. *Biosci Biotechnol Biochem* 2008;72(11):2815–23.
- [26] Shen, L., et al., Ginsenoside Rb1 reduces fatty liver by activating AMP-activated protein kinase in obese rats. *J Lipid Res*. 54(5): p. 1430–1438.
- [27] Srinivasan K, et al. Combination of high-fat diet-fed and low-dose streptozotocin-treated rat: a model for type 2 diabetes and pharmacological screening. *Pharmacol Res* 2005;52(4):313–20.
- [28] Yuan G, Al-Shali KZ, Hegele RA. Hypertriglyceridemia: its etiology, effects and treatment. *CMAJ* 2007;176(8):1113–20.
- [29] Jialal I, Amess W, Kaur M. Management of hypertriglyceridemia in the diabetic patient. *Curr Diab Rep* 2010;10(4):316–20.
- [30] Tomlinson JW, et al. Impaired glucose tolerance and insulin resistance are associated with increased adipose 11beta-hydroxysteroid dehydrogenase type 1 expression and elevated hepatic 5alpha-reductase activity. *Diabetes* 2008;57(10):2652–60.
- [31] Morimoto A, et al. Increase in homeostasis model assessment of insulin resistance (HOMA-IR) had a strong impact on the development of type 2 diabetes in Japanese individuals with impaired insulin secretion: the Saku study. *PLoS One* 2014;9(8):e105827.
- [32] Pataky MW, et al. High-fat diet-induced insulin resistance in single skeletal muscle fibers is fiber type selective. *Sci Rep* 2017;7(1):13642.
- [33] Hancock CR, et al. High-fat diets cause insulin resistance despite an increase in muscle mitochondria. *Proc Natl Acad Sci U S A* 2008;105(22):7815–20.
- [34] Cheng J, et al. Loss of Mbd2 protects mice against high-fat diet-induced obesity and insulin resistance by regulating the homeostasis of energy storage and expenditure. *Diabetes* 2016;65(11):3384–95.
- [35] Enomoto H, et al. Liver fibrosis markers of nonalcoholic steatohepatitis. *World J Gastroenterol* 2015;21(24):7427–35.
- [36] Armutcu F, et al. Markers in nonalcoholic steatohepatitis. *Adv Clin Chem* 2013;61:67–125.
- [37] Regev A, et al. Sampling error and intraobserver variation in liver biopsy in patients with chronic HCV infection. *Am J Gastroenterol* 2002;97(10):2614–8.
- [38] Sharma S, Khalili K, Nguyen GC. Non-invasive diagnosis of advanced fibrosis and cirrhosis. *World J Gastroenterol* 2014;20(45):16820–30.